Talanta 114 (2013) 95–102

Contents lists available at ScienceDirect

Talanta

journal homepage: www.elsevier.com/locate/talanta

$^{1}H–^{13}C$ NMR-based urine metabolic profiling in autism spectrum disorders

Sylvie Mavel [a,*], Lydie Nadal-Desbarats [a,c], Hélène Blasco [a], Frédérique Bonnet-Brilhault [b], Catherine Barthélémy [b], Frédéric Montigny [c], Pierre Sarda [d], Frédéric Laumonnier [a], Patrick Vourc'h [a,c], Christian R. Andres [a], Patrick Emond [a,c]

[a] Université François-Rabelais, INSERM U930, Equipe neurogénétique et neurométabolomique, CHRU de Tours, 10 Bv Tonnellé, 37044 Tours, France
[b] Université François-Rabelais, INSERM U930, Equipe Autisme, CHRU de Tours, 10 Bv Tonnellé, 37044 Tours, France
[c] Université François-Rabelais, PPF "Analyses des Systèmes Biologiques", UFR de Médecine, 10 Bv Tonnellé, 37044 Tours, France
[d] CHRU de Montpellier, hôpital Arnaud-de-Villeneuve, 34295 Montpellier, Cedex 5, France

ARTICLE INFO

Article history:
Received 16 October 2012
Received in revised form
16 March 2013
Accepted 25 March 2013
Available online 9 April 2013

Keywords:
HSQC NMR spectroscopy
Autism spectrum disorders
Urinary metabolites
OPLS-DA
Metabolomics

ABSTRACT

Autism Spectrum Disorders (ASD) are a group of developmental disorders caused by environmental and genetic factors. Diagnosis is based on behavioral and developmental signs detected before 3 years of age with no reliable biological marker. The purpose of this study was to evaluate the potential use of a 2D NMR-based approach to express the global biochemical signature of autistic individuals compared to normal controls. This technique has greater spectral resolution than to 1D ^{1}H NMR spectroscopy, which is limited by overlapping signals. The urinary metabolic profiles of 30 autistic and 28 matched healthy children were obtained using a $^{1}H–^{13}C$ NMR-based approach. The data acquired were processed by multivariate orthogonal partial least-squares discriminant analysis (OPLS-DA). Some discriminating metabolites were identified: β-alanine, glycine, taurine and succinate concentrations were significatively higher, and creatine and 3-methylhistidine concentrations were lower in autistic children than in controls. We also noted differences in several other metabolites that were unidentified but characterized by a cross peak correlation in $^{1}H–^{13}C$ HSQC. Statistical models of ^{1}H and $^{1}H–^{13}C$ analyses were compared and only 2D spectra allowed the characterization of statistically relevant changes [$R^2Y(\text{cum})=0.78$ and $Q^2(\text{cum})=0.60$] in the low abundance metabolites. This method has the potential to contribute to the diagnosis of neurodevelopment disorders but needs to be validated on larger cohorts and on other developmental disorders to define its specificity.

1. Introduction

Autistic disorder (AD), Asperger syndrome (AS) and pervasive developmental disorder-not otherwise specified (PDD-NOS) are collectively termed as autism spectrum disorders (ASD). The prevalence of ASD appears to be increasing (1 in 110 children in 2009) [1] without identification of the etiology of this increase [2–5]. Autism is diagnosed in infancy between the second and the third years of life [6]. Autistic children are particularly characterized by a behavioral triad of impaired communication, impaired social interaction, and restricted and repetitive interests and activities, as listed in the Diagnostic and Statistical Manual of Mental Disorders (DSM-IV). Diagnosis is in part made clinically by subjective analyses based on perceived behaviors in the patient, and is thus dependent on the expertise of those administering the tests. Several studies have explored the possibility of using metabolite profiles to contribute to the diagnosis of developmental disorders [7]. As autism disease has many suspected causes including dysfunctions of the gastrointestinal, immunologic and/or neurologic systems, with some markers showing ubiquitous distribution, it could be assumed that urine metabolites profile could help in the diagnosis and in the pathophysiological mechanisms knowledge of the autism pathology [8,9]. Furthermore urine represents a sample of choice as it is easily and non-invasively collected, that is of particular importance when exploring the autistic population and so we explored in this paper through 2D NMR analysis, the metabolic signature of patients' urine compared to those of healthy subjects in order to identify potential biomarkers useful for the early diagnosis of ASD.

Metabolomics approaches offer the possibility of assessing metabolic signatures linked with genetic and environmental factors. These approaches have previously been applied for disease diagnosis, therapeutics, functional genomics and toxicology studies [10,11]. The most commonly used analytical platforms to identify and quantify metabolites are gas chromatography combined with mass spectroscopy (GC–MS) and nuclear magnetic resonance spectroscopy (NMR) [12–14]. ^{1}H NMR spectroscopy is a powerful, rapid analytical method providing a metabolic profile and has already yielded promising results in diagnosing neuropsychiatric disorders such as autism [7]. Unfortunately, a relatively small number of metabolites can be identified by this method,

* Corresponding author. Tel.: +33 2 47 36 72 40; fax: +33 2 47 36 72 24.
E-mail address: sylvie.mavel@univ-tours.fr (S. Mavel).

0039-9140/$ - see front matter © 2013 Elsevier B.V. All rights reserved.
http://dx.doi.org/10.1016/j.talanta.2013.03.064

as signals were disturbed by spectral overlap. To improve the ability to identify a mixture of components by NMR, two dimensional NMR (2D-NMR) spectra may be of value. Heteronuclear single quantum coherence (^{1}H–^{13}C HSQC)-based NMR provides higher resolution than classical 1D-NMR-based approaches [15–18]. The 2D-NMR HSQC results in a 2D map in which the two axes correspond to a ^{1}H NMR and a ^{13}C-NMR spectrum. Furthermore, 2D-NMR reduces the problem of spectral overlap by peak dispersion and results in a higher proportion of resolved peaks, thus increasing metabolite specificity (for example, between 30 and 50 metabolites can be characterized by ^{1}H NMR [19] compared to more than 150 by HSQC [20] in urine samples). This technique has recently been used in several studies [21–23] to determine plant fingerprinting [17] and animal systems [24], and in human metabolic studies [25,26] but, to our knowledge, the study reported here is the first 2D HSQC-based NMR study applied to the screening of urine samples of ASD patients and controls.

This report evaluates a 2D-NMR-based approach to explore the metabolic profile of urine in an ASD context. As part of this study, statistical analysis methods [principal component analysis (PCA), partial least squares discriminant analysis (PLS-DA) and orthogonal partial least squares discriminant analysis (OPLS-DA)] were used to reveal metabolites that discriminated between ASD and control populations.

2. Materials and methods

2.1. Sample collection

Between 2008 and 2010, urinary samples were collected in sterile vials untreated with preservative from children aged 6–14 years (mean 8 years) with ASD living in France ($n=30$; male 80%, female 20%) and control children ($n=28$; male 61%, female 39%) aged 6–9 years (mean 8 years). All study participants provided informed consent. The severity of autism was assessed according to the International Classification of Diseases 10th Edition during medical consultations in three French autism centers [Tours ($n=11$), Montpellier ($n=15$), and Orléans ($n=4$)] and 28 urine samples from healthy volunteers from Tours. Each urine sample was aliquoted in a 1.5 mL Eppendorf tube and stored at −80 °C immediately after collection until analysis.

2.2. NMR study

2.2.1. Sample preparation

Urine samples were thawed out at room temperature, and centrifuged (at 3000 g) for 10 min. Samples were prepared by mixing 500 μL of urine supernatant, 100 μL of D_2O solution with internal reference [3-trimethylsilylpropionic acid (TSP), 0.05 wt% in D_2O] and 100 μL of phosphate buffer to obtain pH = 7.4 ± 0.5. Samples then were transferred into conventional 5-mm NMR tubes for ^{1}H–^{13}C NMR analysis.

2.2.2. NMR spectroscopy experiments

All NMR experiments were performed at 298 K on a Bruker DPX Avance spectrometer operating at 300 MHz, using a double resonance (^{1}H–^{13}C) 5-mm (Bruker SADIS, Wissembourg, France).

Standard one dimensional (1D) NMR spectra were acquired using a "zgcppr" pulse program in the Bruker library. 32K data points with 16 scans were acquired using a spectral width of 3001 Hz. Water suppression was achieved during the relaxation delay of 2 s using a waltz 16 decoupling sequence with a decoupling power of 55 dB during the acquisition period. All samples were automatically tuned, matched and shimmed.

All sensitivity-enhanced ^{1}H–^{13}C HSQC spectra were collected using an "hsqcetgp" pulse program in the Bruker library with 512 × 128 data points using 32 scans per increment, with acquisition time of 0.0852 s in t_2 with a relaxation time of 2.5 s. The spectral widths were set at 20 ppm in the proton dimension and 250 ppm in the carbon. ^{13}C-decoupling during acquisition was performed using GARP sequence (pulse length 1 ms) applied during t_2. The coupling constant $^1J_{C-H}$ was fixed at 145 Hz, using a shine shaped gradient of 80, 20.1, 20.1, and a homospoil gradient pulse recovery delay of 200 μs. Each experiment lasted 3 h.

2.2.3. Data processing

1D and 2D spectra were processed using MestReNova version 7.1.0 software (Mestrelab Research, S.L., Santiago De Compostela, Spain). After Fourier transformation of each FID, 1D spectra were phased manually. All urine spectra were normalized with an external reference [3-trimethylsilylpropionic acid (TSP), 0.05 wt% in D_2O]. TSP served as a chemical shift reference set at 0 ppm and as a quantitative reference signal. Predefined 2D integration regions were established manually from several spectra (all cross-peaks presented in six controls and in six ASD samples were cumulated). Once this predefined list had been established, HSQC cross-peaks were automatically referenced to the TSP signal, and then were automatically integrated. TSP integration was set at the same value for each spectrum. The region from 4.45 ppm to 5.15 ppm was removed to eliminate baseline effects due to the water signal. The previously established list contained 163 different ^{13}C cross-peaks between 10 and 150 ppm.

The signals were assigned, as far as possible, by comparison with the chemical shifts given by the freely available Metabominer software [20] or from literature data [25], with tolerances of 0.05 ppm (^{1}H) and 0.1 ppm (^{13}C). Identification was achieved if there was only one candidate in the database within the specified tolerances for an observed peak.

All 1D spectra were corrected for phase distortion and the baseline was corrected manually for each spectrum. Two methods of integration were done. The first was an automated "bucketing" with a fixed width of 0.04 ppm per bin. The second method was called "rationalized" integration: 1D proton spectra were prepared as a data matrix by bucket integration from the list obtained from the predefined 2D integration regions. From this predefined 2D auto-integration region, the f2 listing (corresponding to ^{1}H dimension) was retained to define the predefined 1D ^{1}H f1 auto-integration region. Duplicate buckets having the same ^{1}H chemical shift (in f2 listing) were removed. In regions where no ^{1}H–^{13}C cross-peaks were observed, buckets with constant 0.04 ppm width were defined. As the predefined 2D auto-integration region was established manually taking into account each individual signal, allowing signals with different larger shifts, the 186 resulting buckets were so defined with variable widths (but with a mean of 0.05 ppm).

2.3. Statistical methods

The intensity of all peaks for all urine samples was studied by multivariate statistical methods, following protocols given in the literature [27,28].

2.3.1. Multivariate analysis

Multivariate analysis was performed using Simca-P$^+$-12 software (version 12.0, Umetrics, Umeå, Sweden). Unit variance (UV) scaling, pareto scaling (Par), obtained by dividing each variable by the square root of its standard deviation, or logarithmic transformation, which is a nonlinear conversion, were used to minimize the impact of noise or high variability of the variables [29]. Principal component analysis

(PCA) [30] was first performed as an unsupervised clustering to identify the similarity or the differences between sample profiles. Grouping, trends and outliers were revealed from the scatter plot. If these outliers were also detected in the distance to model plot (DModX), which was based on residual variance of the model, they were rejected from the model, and a PCA model was rebuilt. In order to identify subsets (linear combinations) of metabolic features associated with a specific sample class (ASD or control), partial least squares (PLS) analysis was used as supervised clustering. PLS derives latent variables which describe the maximum proportion of covariance between measured data (X matrix) and the response variable (Y matrix) [31]. Orthogonal partial least squares discriminant analysis (OPLS-DA), also used for discrimination, is a refinement of this approach: variation in the data measured is partitioned into two blocks, one containing variations that correlate with the class identifier (ASD or control) and the other containing variations that are orthogonal to the first block and thus do not contribute to discrimination between the defined groups [32]. The quality of the models was described by the cumulative modeled variation in the X matrix R^2X(cum), the cumulative modeled variation in the Y matrix R^2Y(cum), and the cross validated predictive ability Q^2(cum) values. Models were rejected if they presented complete overlap of Q^2 distributions [Q^2(cum) < 0] or low classification rates [Q^2(cum) $<$ 0.05 and eigenvalues should be > 2]. The features with variable importance on projection (VIP) values and regression coefficients |CoeffCS[1]|lower than 0.35 were deleted and evaluated again. A number of variables were obtained from PLS-DA and OPLS-DA that were responsible for the difference between ASD and control urine samples for VIP value > 1.0.

One of the main problems with PLS-DA is the data overfitting occurring if the algorithm picks up random noise to real signals. To validate the model, the data are divided into seven parts, a model is built on 6/7th of data left in, and the left out data are predicted [33]. The predicted data are then compared with the original data and the sum of squared errors calculated for the whole dataset. This is converted into Q^2, which is an estimation of the predictive ability of the model. The model was thus considered sufficiently well guarded against overfitting and validated after 200 random permutation tests [34] as the Q^2 line intercepted the Y axis at a negative value.

Furthermore, we also performed PLS-DA with autoscaling normalization which is very similar to pareto scaling using the freely available web-based software called MetaboAnalyst [20].

2.3.2. Univariate analysis

Student's t-test was performed using MetaboAnalyst [20] for all metabolites with a VIP > 1.0. The ratio of the peak areas of these metabolites to that of creatinine was calculated and a non-parametric test was performed with the critical p-value set at 0.05 [28,35].

3. Results

3.1. NMR Experiments

A typical 2D HSQC spectrum of urine fitted with the ^{1}H NMR sub-spectrum on its side is shown in Fig. 1. The 2D-HSQC analysis provided 163 cross-peaks integrated and normalized with an external reference (TSP).

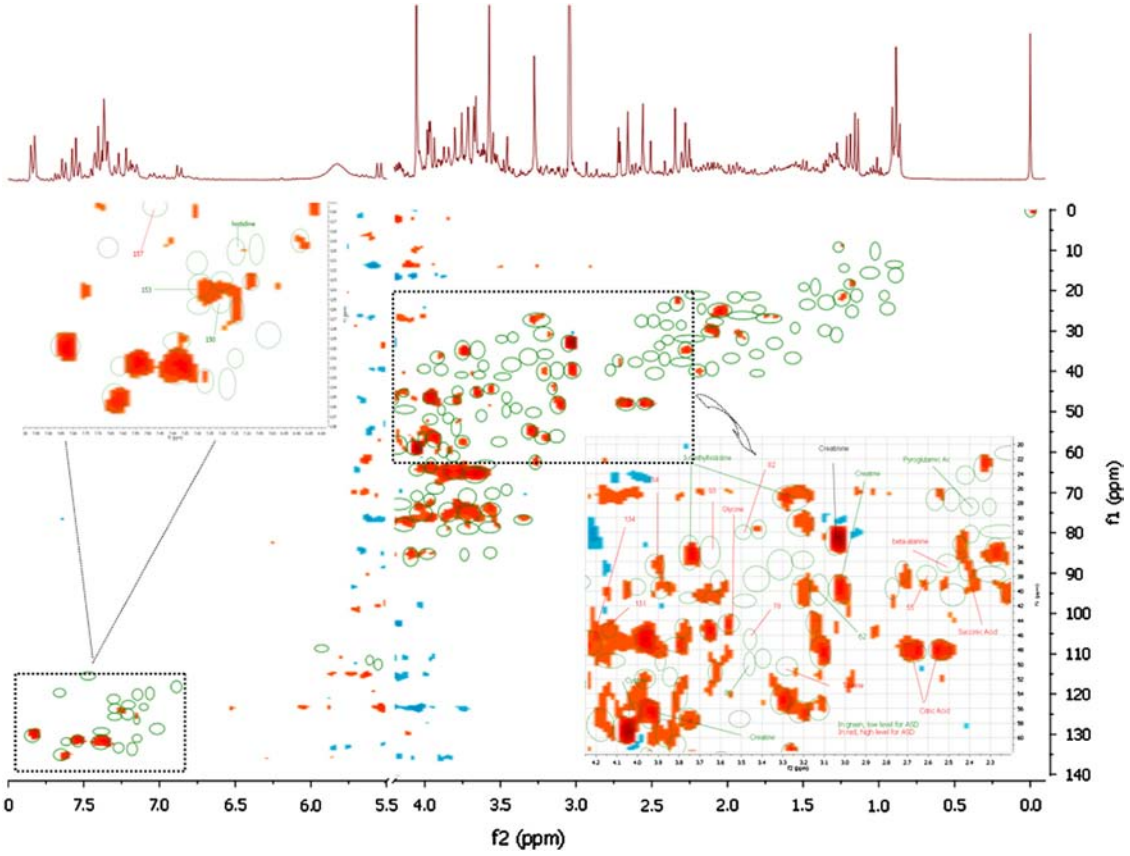

Fig. 1. ^{1}H–^{13}C HSQC NMR spectrum of urine at 300 MHz, with a typical ^{1}H spectrum as external spectrum, showing the assignment of the significant metabolites responsible for discriminating children with ASD from non-autistic children when possible. Only VIP > 1 obtained by OPLS-DA (model 4) were distinguished. Peaks increased in the ASD group are in red, and those decreased are in green. (For interpretation of the references to color in this figure caption, the reader is referred to the web version of this article.)

3.2. Statistical studies from 2D HSQC NMR data – choice of pre-treatment technique

PCA was performed as unsupervised clustering and we did not identify any particular similarity or any great differences between sample profiles (no outliers were eliminated). Discriminating metabolites were proposed using PLS-DA and OPLS-DA from one predictive and two or more orthogonal components. We have studied the impact of pre-treatment of the NMR data before multivariate analysis using unit variance (UV), pareto (Par), and autoscaling. In parallel, the impact of log-based transformation was performed.

Table 1 summarizes the features of the different models. The processed variables are represented by *X* (metabolites), *Y* variables represent the different children's urine samples. R^2X(cum) is the sum of predictive orthogonal variations in *X* that is explained by the model. From the predictive variation between *X* and *Y* given by R^2X (cum), models 1 and 2 with the same scaling (UV) interpreted around 30% of the total variation in X (0.29 and 0.27, respectively, Table 1). The amount variation that could not be explained by the model might originate from the noise. This variation was minimized by Pareto scaling and for model 3 is expressed by the formula [36]: $1-R^2X-R^2X(\text{cum})=1-0.0593-0.598=0.343$, as noise could account for 34% in this analysis. The quality of the models was expressed by R^2Y(cum) and Q^2(cum) values, where R^2Y(cum) is defined as the proportion of variance in the data explained by the models and indicates goodness of fit. All the models explained around 70–80% of the variations in the different peaks. A high Q^2(cum) value [Q^2(cum) >0.5] indicated good predictivity. Table 1 shows that noise was minimized by Pareto scaling [R^2X(cum) higher in models 3], but this pre-treatment led to lower predictability [Q^2(cum)=0.43]. As UV scaling seemed to be the best scaling in our study (confirmed by analysis of variance CV-ANOVA, *p*-value=7.773.e–009, see supporting information), we focused on this method. Thus the OPLS-DA cross-validated score plots for model 2 (Fig. 2) showed discrimination between the two populations.

Table 1
Summary of statistical values of PLS-DA and OPLS-DA of ^{1}H–^{13}C HSQC with different data scaling. The different cumulated modeled variations in *X* [R^2X (cum)) and *Y* (R^2Y(cum)] matrices on spectral datasets and predictability of the model (Q^2) are given [observations (N)=58].

	Scaling/ transformation	R^2X	R^2X (cum)	R^2Y (cum)	Q^2 (cum)
Model 1[a]	UV	0.0533	0.290	0.784	0.399
Model 2[b]	UV	0.0488	0.271	0.782	0.602
Model 3[c]	Pareto	0.0593	0.598	0.700	0.428
Model 4[d]	Log transformed, UV scaling	0.0525	0.155	0.758	0.544

[a] PLS-DA, from 3 components, Variables *X*=63.
[b] OPLS-DA, Variables *X*=43, 2 orthogonal projections.
[c] OPLS-DA, Variables *X*=54, 3 orthogonal projections.
[d] OPLS-DA, , Variables *X*=44, 1 orthogonal projection.

3.3. Statistical studies from 2D HSQC NMR data – analysis of model and identification of important features

From PLS-DA or OPLS-DA, the most highly contributing metabolites in the discrimination of the two populations were screened recording to the variable importance on projection (VIP) values >1.0. The effect of a data pre-treatment method on the ranking of the metabolites is presented in Table 2. For example, a signal characterized by peak ID 123 was identified as the most relevant for PLS-DA and OPLS-DA methods using UV scaling, or log transformed, but was the 6th rank with Pareto scaling (Table 2, model 3). As another example, pyroglutamic acid (peak ID 46) was the 6th highest metabolite on OPLS-DA UV scaling, while by log transformation, pyroglutamic acid appeared after the first 15 most relevant metabolites when applying rank scaling. The differences could be due to the magnitude of the fold change (or relative standard deviation) of some metabolites present that was balanced by nonlinear log transformation. Furthermore, a PLS model, with autoscaling normalization, was also tested and provided the same VIP as shown in Table 2 (model 5).

The loading scatter plot in Fig. 3 shows which variables led to discrimination between ASD and control children in model 2 (Table 1), the chosen model.

The results of discriminating biomarkers were validated using univariate analysis (Student's *t*-test) calculated as the ratio of the selected urinary metabolite peak area to creatinine. We obtained seven cross-peaks (Table 2) with significant differences at $p<0.05$.

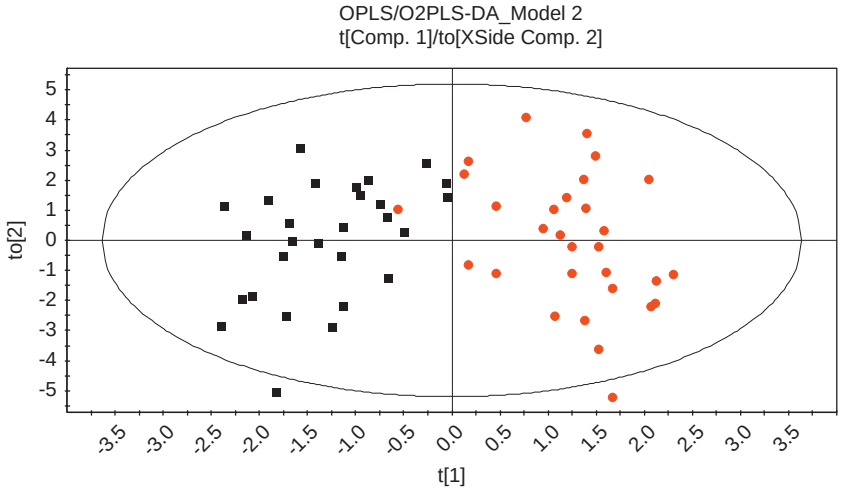

Fig. 2. Scatter plot of OPLS-DA scores of the first principal component obtained from ^{1}H–^{13}C HSQC NMR spectra of urine samples, model 2 (UV scaling, Table 1) [(n=30 ASD samples (red dot), n=28 control samples (black box) with R^2Y(cum)=0.78 and Q^2(cum)=0.60]. (For interpretation of the references to color in this figure caption, the reader is referred to the web version of this article.)

Table 2
Analysis of urinary metabolites in children: cross-peak and chemical shift values for 2D ^{1}H–^{13}C HSQC spectra and variable importance (VIP values) for different statistical studies.

Peak	^{1}H (ppm)	^{13}C (ppm)	Differentiation for ASD samples	Potential assignment	PLS-DA.VIP coeff		OPLS-DA.VIP coeff[a]		
					UV[a] Model 1	Autoscaling[b] Model 5	UV Model 2	Pareto Model 3	Log transformed,UV Model 4
123	4.01	56.67	↓	Cystathionine/Cystine [c]	1.77	2.28 *(0.0082)*	1.66	1.43	1.66
157	7.47	115.5	↑	Indican/Serotonin [c]	1.60	2.18	1.58	< 1	1.60
56	2.67	48.35	↑	Citric acid	1.54	1.94 *(0.0464)*	1.56	2.08	1.31
134	4.24	47.08	↑	ND	1.47	2.12 *(0.0570)*	1.54	1.77	1.50
100	3.75	34.76	↓	3-Methylhistidine	1.39	1.89 *(0.0438)*	1.37	2.36	1.33
46	2.40	28.51	↓	Pyroglutamic acid	1.32	1.86	1.34	–	1.04
116	3.94	56.81	↓	Creatine	1.41	1.85 *(0.0447)*	1.34	2.79	1.04
82	3.49	31.99	↑	3-Methylxanthine/…. [c]	1.30	1.84	1.33	< 1	1.41
78	3.46	46.57	↑	Homovanillic ac/4-hydroxy phenyl acetic [c]	1.29	1.82	1.32	< 1	1.20
131	4.14	45.36	↑	ND	1.23	1.76	1.28	< 1	1.31
138	5.56	112.65	↑	ND	1.21	1.74	1.26	< 1	–
47	2.42	36.96	↑	Succinic acid	1.28	1.73	–	< 1	1.22
128	4.09	85.92	↑	Cytidine/ [c]	1.17	1.65	1.20	1.21	< 1
52	2.51	36.23	↑	*β*-alanine	1.15	1.60	–	< 1	1.22
80	3.46	49.88	↓	ND	1.15	1.58	1.15	< 1	1.08
93	3.65	34.72	↑	ND	1.14	1.58	1.14	1.02	0.97
77	3.43	38.34	↑	Taurine/dihydrouracil [c]	1.11	1.32	0.95	< 1	1.30
55	2.61	37.75	↑	ND	–	1.55 *(0.0478)*	–	< 1	< 1
85	3.56	44.40	↑	Glycine	1.08	1.52	–	1.46	1.03
114	3.92	36.57	↑	ND	1.03	1.44	1.05	0.99	< 1
62	3.13	39.81	↓	Tyrosine /Phenylalanine/…[c]	1.10	1.44	1.05	< 1	1.03
145	7.14	120.12	↓	Histidine	1.07	1.39 *(0.0173)*	1.00	< 1	1.10
150	7.21	125.00	↓	Tryptophan/Indolacetic acid [c]	1.04	1.30 *(0.0343)*	0.94	< 1	< 1
70	3.28	50.25	↑	Taurine	1.02	0.90	< 1	< 1	–
153	7.30	125.62	↑	Indican/…[c]	0.98	1.37	1.00	< 1	1.05

(↑) denotes an increased concentration for ASD population, (↓): decreased.
(ND) data not determined.
(–) denotes not present in the model.
[a] Magnitude of variation of VIP with a threshold of 1.0 obtained using Simca-P^{+} software.
[b] VIP values obtained from MetaboAnalyst software, *p*-value given in brackets and italics after ratio of peak areas to creatinine.
[c] denotes ambiguity in the characterization.

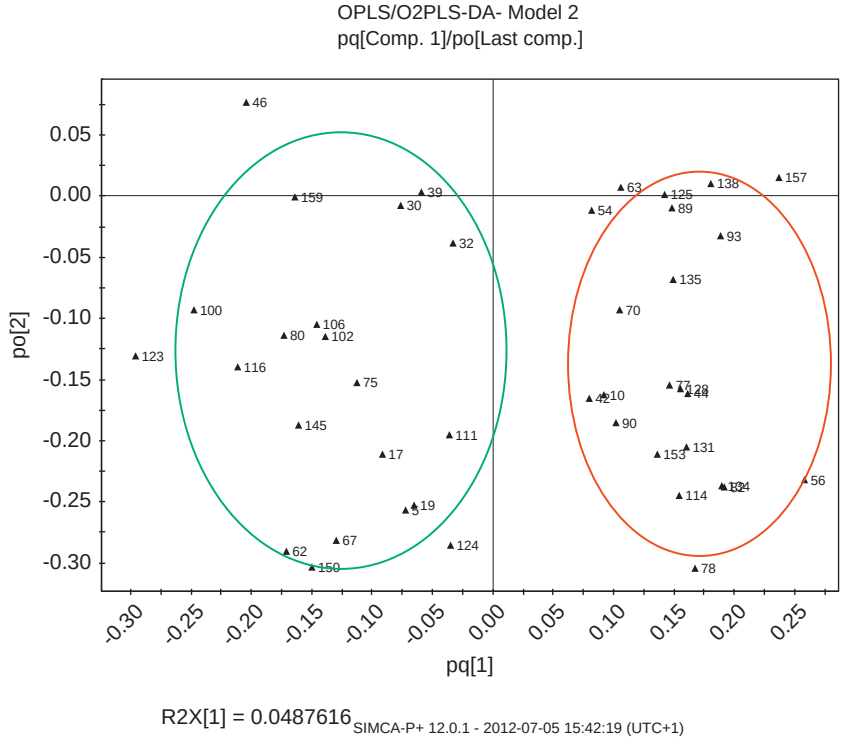

Fig. 3. pq loading plot of OPLS-DA model 2 (Table 1): scatter Plot of the X- and Y-loadings (p and q). This plot shows how the responses (Y's) varied in relation to each other, i.e. which provided similar information and their relationship to the terms of the model. Two tendencies could be seen. Peaks framed in red were higher levels in ASD urine, and peaks framed in green were lower. (For interpretation of the references to color in this figure caption, the reader is referred to the web version of this article.)

3.4. Targeted segmentation of ^{1}H-NMR spectra using a priori 2D HSQC cross-peaks

As NMR spectral data from a 600 MHz spectrometer were statistically more relevant compared to our spectral data obtained at 300 MHz, we expected that from results obtained from 2D study, we could improve the analysis of ^{1}H NMR data obtained on a low field spectrometer. Once the 2D HSQC NMR spectra had been analyzed by multivariate data analysis, targeted metabolic segmentation was performed on the ^{1}H NMR spectra to improve the usual automated ^{1}H NMR segmentation. The 1D segments were established using the 2D integration zones, taking into account each individual signal allowing signals with larger shifts. This resulted into variable width integration areas, with a mean width of 0.05 ppm. PLS-DA showed that this "rational" segmentation, which was more time consuming, resulted in a slightly better model (Table 3, model 6), 47% of the proportion of variance of the data obtained from variable widths being explained by PLS-DA compared to 42% [R^2Y(cum)= 0.42] obtained from the automated fixed width of 0.04 ppm per bin. The cross-validated predictive ability Q^2(cum) values were slightly better for the "rationalized" method compared to the automated "bucketing" method (0.24 compared to 0.17, respectively). Even with "rationalized" method, compared to Yap et al.'s study [7], PLS-DA study of ^{1}H NMR spectral data was statistically more relevant using a 600 MHz spectrometer compared to our spectral data obtained at 300 MHz [R^2Y(cum)=0.72 and Q^2(cum)=0.33 [7] compared to 0.475 and 0.24, respectively, in model 6 (Table 3)].

To improve the discrimination analysis of ^{1}H NMR-300 MHz data on targeted metabolites, OPLS-DA was performed following the same pre-treatment procedure as the 2D study. For this 1D study, the quality of OPLS-DA with regard to R^2X(cum) and R^2Y (cum) values showed that UV (Table 3, model 7) and pareto (Table 3, model 8) scaling led to the same discrimination [0.55 ± 0.01 for R^2X(cum) and 0.46 for R^2Y(cum)], log transformation (Table 3, model 9) provided a weaker result with R^2Y(cum)= 0.40. In terms of the predictability of the different models, UV scaling seemed to be the best with Q^2(cum)=0.32 compared to less than 0.20 for the other two OPLS-DA (Table 3, models 8 and 9). Using the same NMR spectrometer (300 MHz), the multivariate analysis on targeted metabolites was clearly better for 2D NMR analysis compared to 1D NMR analysis. With UV scaling, model 7 only explained 46% of the variations in the different peaks [R^2Y (cum)=0.458] compared to 78% for model 2 (Table 1) in the 2D analysis. The predictability regarding Q^2(cum) values was also much better in the 2D study (0.59 for model 2 compared to 0.32 in model 7).

Table 3
Summary of PLS-DA and OPLS-DA of ^{1}H statistical values with different data scaling. The different cumulated modeled variations in X [R^2X(cum)] and Y [R^2Y (cum)] matrix on spectral datasets and predictability of the model (Q^2) are given [observations (N)=58].

	Scaling/ transformation	R^2X	R^2X (cum)	R^2Y (cum)	Q^2 (cum)
Model 6[a]	UV	0.173	0.539	0.475	0.24
Model 7[b]	UV	0.086	0.561	0.458	0.32
Model 8[c]	Pareto	0.0505	0.543	0.462	0.193
Model 9[d]	Log transformed, UV scaling	0.123	0.755	0.406	0.217

[a] PLS-DA, from 3 components, Variables X=51.
[b] OPLS-DA, Variables X=43, 2 orthogonal projections.
[c] OPLS-DA, Variables X=65, 2 orthogonal projections.
[d] OPLS-DA, Variables X=34, 3 orthogonal projections.

4. Discussion

A metabolomics approach using 2D-NMR is a powerful tool to analyze rich biological fluid such as urine. A 2D-NMR spectrum provides more information compared to a 1D-NMR spectrum as one peak is obtained for each pair of coupled nuclei, whose two coordinates are the chemical shifts of the two coupled atoms. When a HSCQ sequence is used, correlation peaks show the connectivity between carbons (^{13}C) and their attached protons. Although a 2D-NMR strategy is more time consuming than ^{1}H-NMR, it provides a more detailed picture of the matrix composition especially in resonance areas where overlapping occurs. Fewer overlapping problems are seen in ^{13}C-NMR spectra because of the larger chemical shift dispersion (200 ppm compared to 10 ppm for ^{1}H). In 2D spectra, peaks from low abundance structures are better resolved from neighboring peaks belonging to more abundant structures, and thus can be characterized when 1D ^{1}H-NMR analysis cannot resolve overlapping signals because the more abundant structures may hide less abundant metabolites.

Metabolomics studies using ^{1}H NMR-based applications have shown variations in urinary metabolic profiles between children with and without ASD [7]. As this previous study analyzed around 20 metabolites, we expected that 2D spectra would improve the identification of statistically relevant changes in the abundance metabolites. Data processing methods are highly dependent on the pre-treatment technique of these values. Variations between samples can generally be classified into "technical" or "biological" variance, but the impact of technical variability should be minimized and discrimination of noise from useful biological data obtained. Several types of scaling are usually used: UV, Par, and autoscaling. UV means that the variable is centered and scaled from the standard deviation of the variable. The combination of scaling and mean centering is called autoscaling in MetaboAnalyst software [each descriptor (with high or small intensity) is weighted equally] [37]. In Par scaling, which is similar, the variance changes from variable to variable, but the range of variance across each spectrum is much reduced from the initial unscaled data (weak values being scaled up while the stronger intensities are scaled down). The choice of pre-treatment methods depends on several factors (numbers of samples, magnitude of concentration, similarities, etc), and emphasizes different aspects of the data. As each method has its own merits and drawbacks, and as, to our knowledge, no-one has determined what the best pre-treatment is for NMR-based data in children's urine, we studied the impact of these scaling methods on identification of biomarkers.

We found that pre-treatment affected the ranking of the data, but the listing without ranking for all VIP >1.0 was almost the same whatever the pre-treatment used. UV scaling seemed to be the best scaling method for our study. As OPLS-DA is recommended to obtain a clearer and more straightforward interpretation [37], we focused on this method. As UV scaling is usually used, and in order to be able to compare our results with other studies [7], and as the types of other scaling did not lead to better interpretation, we focused on results obtained from OPS-DA using UV scaling (Table 1, model 2).

Factors such as disease, drugs and diet are known to modify individual metabolites concentrations [38,39]. Furthermore, the number of samples studied was too limited to obtain any real statistical characterization of a general population of children. Nevertheless, it may be useful to explore whether certain tendencies (characterized or unknown peaks) can be detected in the samples studied. Few untargeted metabolomics studies have been performed on urine samples to identify biomarkers of ASD [7,40]. A previous OPLS-DA (UV scaling) showed that the profile of urinary metabolites was not so easy to analyze by ^{1}H NMR spectroscopy [weak R^2Y

(cum)=0.275 and Q^2(cum)=0.15] [7]. Using 2D HSQC analysis we obtained a group with improved statistical significance in the model's predictability [R^2Y(cum)=0.78 and Q^2(cum)=0.60]. As previously described [7,40], we found (Table 2) an increase in β-alanine, glycine, taurine and succinate concentrations in the ASD group. However, glutamate, formate, dimethylamine, trimethylamine *N*-oxide and hippurate were not found to provide any discrimination between our two populations (VIP «1, see supplementary information). This may be explained by the improved resolution of 2D NMR spectra leading to more precise determination of relevant peaks, and a greater number of correlated variables, as VIP is a cumulative vector over all components up to the selected one. As in Yap et al.'s study [7], the metabolites that were significantly lower for the ASD children were creatine and 3-methylhistidine. However, in contrast, in their study, *N*-methylnicotinamide and *N*-methylnicotinic acid were not observed in the aromatic zone, and for aliphatic protons, chemical shifts were outside our range of study (region near water saturation).

The listing of these potent biomarkers went in the same way as previous results obtained by GC/flame ionization detection (FID) analysis: cystine, histidine, tryptophan, and phenylalanine were also in lower concentrations in autistic group [41]. Kaluzna-Czaplinska et al. have studied by GC–MS urine of autistic children and have described, as shown in this 2D NMR study, an increase in urine of autistic children of citric acid [42], and homovanillic acid [43] concentrations, and a decrease in tryptophan concentration [44]. Serotonin and β-alanine have been shown in increase concentration in autistic population by different metabolomics studies [8].

The results of discriminating biomarkers were validated using univariate analysis. One of the main problems of ^{1}H NMR metabolomics studies is the lack of significance of the data due to the high degree of variability leading to high confidence levels of metabolite concentrations. In a previous 1D ^{1}H NMR study, after *t*-test analysis, the putative biomarkers were not found to be statistically significant [7]. Using 2D NMR study, we obtained seven cross-peaks (Table 2) with significant differences at $p<0.05$ possibly explained by the better selectivity of the technique.

Compared to this previous 1D ^{1}H NMR study [7], where about 10 metabolites were proposed, our 2D HSQC analysis was able to identify 20 discriminating features (VIP > 1) some of which were assigned and others only characterized by their ^{1}H–^{13}C chemical shifts (Table 2). Peaks 93, 114, 123, 131, 134, and 138 were at higher levels in the ASD group than in controls. All these cross-peaks should be assigned more precisely by further studies.

In this study we showed that 2D HSQC-based NMR analysis was able to discriminate between two populations based on their urinary profiles. As many metabolites share several common pathways, and because we evaluated the value of a 300 MHz magnet for metabolomics study, we only focused on the description of the differences between statistically significant metabolites. However further studies are necessary to define the specificity and sensitivity of the parameters identified.

5. Conclusion

Urinary screening by NMR spectroscopy for children with neurodevelopment disorders such as autism could be a good, non-invasive, and easy tool to assess metabolic modifications associated with the disorder. Compared to ^{1}H NMR, 2D HSQC NMR provides the opportunity to burst through potentially overlapping signals in the ^{13}C dimension, increasing the number of peaks and thus the chance to discriminate between populations with different metabolite profiles. Combining NMR spectroscopy with multivariate statistical analysis, we were able to discriminate between a group of 30 ASD children and a group of typically developing children on the basis of their urinary profiles more effectively using 2D ^{1}H–^{13}C HSQC urinary profiles. Pre-processing data is a critical step in the metabolomics workflow. Different scaling methods were evaluated in order to obtain the best statistical model. In this study, we showed that a 2D HSQC sequence done on a widely available 300 MHz spectrometer could be suitable for metabolomics studies. Moreover, although 2D NMR is a little more time consuming, NMR HSQC analysis on targeted metabolites of urine samples is a potentially useful clinical tool for diagnosis of children with ASD compared to non-autistic children and may improve the understanding of the pathogenesis of ASD.

Acknowledgments

This work was supported by the “Institut National de la Santé et de la Recherche” INSERM and the University François-Rabelais. We thank the center “Sésame Autisme Loiret” for their participation to this study. We thank the “Département d'Analyses Chimiques et S. R.M. Biologique et Médicale” (PPF, Tours, France) for chemical analyses.

Appendix A. Supporting information

Supplementary data associated with this article can be found in the online version at http://dx.doi.org/10.1016/j.talanta.2013.03.064.

References

[1] K. Weintraub, Nature 479 (2011) 22–24.
[2] T. Falck-Ytter, C. von Hofsten, Prog. Brain Res. 189 (2011) 209–222.
[3] B. Franke, S.V. Faraone, P. Asherson, J. Buitelaar, C.H. Bau, J.A. Ramos-Quiroga, E. Mick, E.H. Grevet, S. Johansson, J. Haavik, K.P. Lesch, B. Cormand, A. Reif, Mol. Psychiatry 17 (2012) 960–987.
[4] J.C. McPartland, M. Coffman, K.A. Pelphrey, Curr. Opin. Pediatr. 23 (2011) 628–632.
[5] G.B. Schaefer, R.E. Lutz, Genet. Med. 8 (2006) 549–556.
[6] I. Kolvin, Br. J. Psychiatry 118 (1971) 381–384.
[7] I.K. Yap, M. Angley, K.A. Veselkov, E. Holmes, J.C. Lindon, J.K. Nicholson J. Proteome Res. 9 (2010) 2996–3004.
[8] H.V. Ratajczak, J. Immunotoxicol. 8 (2011) 80–94.
[9] L. Wang, M.T. Angley, J.P. Gerber, M.J. Sorich, Biomarker 16 (2011) 537–552.
[10] K. Suhre, S.Y. Shin, A.K. Petersen, R.P. Mohney, D. Meredith, B. Wagele, E. Altmaier, P. Deloukas, J. Erdmann, E. Grundberg, C.J. Hammond, M.H. de Angelis, G. Kastenmuller, A. Kottgen, F. Kronenberg, M. Mangino, C. Meisinger, T. Meitinger, H.W. Mewes, M.V. Milburn, C. Prehn, J. Raffler, J.S. Ried, W. Romisch-Margl, N.J. Samani, K.S. Small, H.E. Wichmann, G. Zhai, T. Illig T.D. Spector, J. Adamski, N. Soranzo, C. Gieger, Nature 477 (2011) 54–60.
[11] J.H. Wang, J. Byun, S. Pennathur, Semin. Nephrol. 30 (2010) 500–511.
[12] T. Gebregiworgis, R. Powers, Comb. Chem. High Throughput Screening 15 (2012) 595–610.
[13] G. Nicholson, M. Rantalainen, A.D. Maher, J.V. Li, D. Malmodin, K.R. Ahmadi, J. H. Faber, I.B. Hallgrimsdottir, A. Barrett, H. Toft, M. Krestyaninova, J. Viksna, S. G. Neogi, M.E. Dumas, U. Sarkans, C. The Molpage, B.W. Silverman, P. Donnelly, J.K. Nicholson, M. Allen, K.T. Zondervan, J.C. Lindon, T.D. Spector, M. I. McCarthy, E. Holmes, D. Baunsgaard, C.C. Holmes, Mol. Syst. Biol. 7 (2011) 525.
[14] G.J. Patti, O. Yanes, G. Siuzdak, Nat. Rev. Mol. Cell. Biol. 13 (2012) 263–269.
[15] J. McKenzie, A. Charlton, J. Donarski, A. MacNicoll, J. Wilson, Metabolomics 6 (2010) 574–582.
[16] W. Gronwald, M.S. Klein, H. Kaspar, S.R. Fagerer, N. Nurnberger, K. Dettmer, T. Bertsch, P.J. Oefner, Anal. Chem. 80 (2008) 9288–9297.
[17] I.A. Lewis, S.C. Schommer, B. Hodis, K.A. Robb, M. Tonelli, W.M. Westler, M. R. Sussman, J.L. Markley, Anal. Chem. 79 (2007) 9385–9390.
[18] R.K. Rai, P. Tripathi, N. Sinha, Anal. Chem. 81 (2009) 10232–10238.
[19] P. Mercier, M.J. Lewis, D. Chang, D. Baker, D.S. Wishart, J. Biomol. NMR 49 (2011) 307–323.
[20] J. Xia, T.C. Bjorndahl, P. Tang, D.S. Wishart, BMC Bioinformatics 9 (2008) 507.
[21] M.E. Dumas, C. Canlet, F. Andre, J. Vercauteren, A. Paris, Anal. Chem. 74 (2002) 2261–2273.
[22] R.K. Rai, N. Sinha, Anal. Chem. 84 (2012) 10005–10011.
[23] M. Zheng, P. Lu, Y. Liu, J. Pease, J. Usuka, G. Liao, G. Peltz, Bioinformatics 23 (2007) 2926–2933.
[24] E. Chikayama, M. Suto, T. Nishihara, K. Shinozaki, J. Kikuchi, PLoS One 3 (2008) e3805.

[25] W. Gronwald, M.S. Klein, R. Zeltner, B.D. Schulze, S.W. Reinhold, M. Deutschmann, A.K. Immervoll, C.A. Boger, B. Banas, K.U. Eckardt, P.J. Oefner, Kidney Int. 79 (2011) 1244–1253.
[26] J. Yuk, J.R. McKelvie, M.J. Simpson, M. Spraul, A.J. Simpson, Environ. Chem. 7 (2010) 524–536.
[27] E.C. Chan, K.K. Pasikanti, J.K. Nicholson, Nat. Protoc. 6 (2011) 1483–1499.
[28] J. Xia, D.S. Wishart, Nat. Protoc. 6 (2011) 743–760.
[29] R.A. van den Berg, H.C. Hoefsloot, J.A. Westerhuis, A.K. Smilde, M.J. van der Wer, BMC Genomics 7 (2006) 142–157.
[30] E.K. Kemsley, G. Le Gall, J.R. Dainty, A.D. Watson, L.J. Harvey, H.S. Tapp I.J. Colquhoun, Br. J. Nutr. 98 (2007) 1–14.
[31] S. Wold, M. Sjöström, L. Eriksson, Chemometr. Intell. Lab. 58 (2001) 109–130.
[32] J. Trygg, J. Chemometr. 16 (2002) 283–293.
[33] O. Cloarec, M.E. Dumas, J. Trygg, A. Craig, R.H. Barton, J.C. Lindon, J. K. Nicholson, E. Holmes, Anal. Chem. 77 (2004) 517–526.
[34] J. Westerhuis, H. Hoefsloot, S. Smit, D. Vis, A. Smilde, E. van Velzen, J. van Duijnhoven, F. van Dorsten, Metabolomics 4 (2008) 81–89.
[35] J. Xia, N. Psychogios, N. Young, D.S. Wishart, Nucleic Acids Res. 37 (2009) W652–W660.
[36] SIMCA-P+ 12 User Guide ⟨http://www.umetrics.com/⟩.
[37] J. Trygg, E. Holmes, T. Lundstedt, J. Proteome Res. 6 (2007) 469–479.
[38] S. Krug, G. Kastenmüller, F. Stückler, M.J. Rist, T. Skurk, M. Sailer, J. Raffler, W. Römisch-Margl, J. Adamski, C. Prehn, T. Frank, K.-H. Engel, T. Hofmann, B. Luy, R. Zimmermann, F. Moritz, P. Schmitt-Kopplin, J. Krumsiek, W. Kremer, F. Huber, U. Oeh, F.J. Theis, W. Szymczak, H. Hauner, K. Suhre, H. Daniel, FASEB J. 26 (2012) 2607–2619.
[39] T. Rosenling, M.P. Stoop, A. Attali, H. Aken, E. Suidgeest, C. Christin, C. Stingl, F. Suits, P. Horvatovich, R.Q. Hintzen, T. Tuinstra, R. Bischoff, T.M. Luider J. Proteome Res. 11 (2012) 2048–2060.
[40] J.K. Nicholson, I.K.S. Yap, E. Holmes, J.C. Lincoln, (2011) from PCT Int. Appl. WO 2011010104 A1 20110127.
[41] C. Evans, R.H. Dunstan, T. Rothkirch, T.K. Roberts, K.L. Reichelt, R. Cosford, G. Deed, L.B. Ellis, D.L. Sparkes, Nutr. Neurosci. 11 (2008) 9–17.
[42] J. Kaluzna-Czaplinska, Clin. Biochem. 44 (2011) 686–691.
[43] J. Kaluzna-Czaplinska, E. Socha, J. Rynkowski, Med. Sci. Monit. 16 (2010) CR445–CR450.
[44] J. Kaluzna-Czaplinska, M. Michalska, J. Rynkowski, Med. Sci. Monit. 16 (2010) CR488–CR492.